

University of Groningen

High yield production of human invariant chain CD74 constructs fused to solubility-enhancing peptides and characterization of their MIF-binding capacities

Go, Tjie Kok; Wasiel, Anna A; Dekker, Frans; Poelarends, Gerrit; Cool, Robbert

Published in:
Protein Expression and Purification

DOI:
[10.1016/j.pep.2018.03.008](https://doi.org/10.1016/j.pep.2018.03.008)

IMPORTANT NOTE: You are advised to consult the publisher's version (publisher's PDF) if you wish to cite from it. Please check the document version below.

Document Version
Version created as part of publication process; publisher's layout; not normally made publicly available

Publication date:
2018

[Link to publication in University of Groningen/UMCG research database](#)

Citation for published version (APA):

Kok, T., Wasiel, A. A., Dekker, F. J., Poelarends, G. J., & Cool, R. H. (2018). High yield production of human invariant chain CD74 constructs fused to solubility-enhancing peptides and characterization of their MIF-binding capacities. *Protein Expression and Purification*. DOI: 10.1016/j.pep.2018.03.008

Copyright

Other than for strictly personal use, it is not permitted to download or to forward/distribute the text or part of it without the consent of the author(s) and/or copyright holder(s), unless the work is under an open content license (like Creative Commons).

Take-down policy

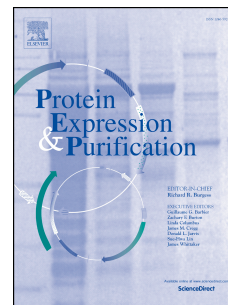
If you believe that this document breaches copyright please contact us providing details, and we will remove access to the work immediately and investigate your claim.

Downloaded from the University of Groningen/UMCG research database (Pure): <http://www.rug.nl/research/portal>. For technical reasons the number of authors shown on this cover page is limited to 10 maximum.

Accepted Manuscript

High yield production of human invariant chain CD74 constructs fused to solubility-enhancing peptides and characterization of their MIF-binding capacities

Tjie Kok, Anna A. Wasiel, Frank J. Dekker, Gerrit J. Poelarends, Robbert H. Cool



PII: S1046-5928(17)30652-6

DOI: [10.1016/j.pep.2018.03.008](https://doi.org/10.1016/j.pep.2018.03.008)

Reference: YPREP 5240

To appear in: *Protein Expression and Purification*

Received Date: 26 October 2017

Revised Date: 19 March 2018

Accepted Date: 22 March 2018

Please cite this article as: T. Kok, A.A. Wasiel, F.J. Dekker, G.J. Poelarends, R.H. Cool, High yield production of human invariant chain CD74 constructs fused to solubility-enhancing peptides and characterization of their MIF-binding capacities, *Protein Expression and Purification* (2018), doi: 10.1016/j.pep.2018.03.008.

This is a PDF file of an unedited manuscript that has been accepted for publication. As a service to our customers we are providing this early version of the manuscript. The manuscript will undergo copyediting, typesetting, and review of the resulting proof before it is published in its final form. Please note that during the production process errors may be discovered which could affect the content, and all legal disclaimers that apply to the journal pertain.

High yield production of human invariant chain CD74 constructs fused to solubility-enhancing peptides and characterization of their MIF-binding capacities

Tjie Kok^{1,2}, Anna A. Wasiel¹, Frank J. Dekker¹, Gerrit J. Poelarends¹ and Robbert H. Cool¹

¹*Department of Chemical and Pharmaceutical Biology, Groningen Research Institute of Pharmacy, University of Groningen, Antonius Deusinglaan 1, 9713 AV Groningen, The Netherlands.*

²*Faculty of Biotechnology, University of Surabaya, Jalan Raya Kalirungkut Surabaya, 60292, Indonesia.*

Dr. R.H. Cool

*University of Groningen, Department of Chemical and Pharmaceutical Biology
Antonius Deusinglaan 1, 9713 AV Groningen, The Netherlands
phone +31 50 36 34321
email: r.h.cool@rug.nl*

Abstract

The HLA class II histocompatibility antigen gamma chain, also known as HLA-DR antigen-associated invariant chain or CD74, has been shown to be involved in many biological processes amongst which antigen loading and transport of MHC class II molecules from the endoplasmic reticulum to the Golgi complex. It is also part of a receptor complex for Macrophage Migration Inhibitory Factor (MIF), and participates in inflammatory signaling. The inhibition of MIF-CD74 complex formation is regarded as a potentially attractive therapeutic target in inflammation, cancer and immune diseases. In order to be able to produce large quantities of the extracellular moiety of human CD74, which has been reported to be unstable and protease-sensitive, different constructs were made as fusions with two solubility enhancers: the well-known maltose-binding domain and Fh8, a small protein secreted by the parasite *Fasciola hepatica*. The fusion proteins could be purified with high yields from *Escherichia coli* and were demonstrated to be active in binding to MIF. Moreover, our results strongly suggest that the MIF binding site is located in the sequence between the transmembrane and the membrane-distal trimerisation domain of CD74, and comprises at least amino acids 113-125 of CD74.

Key words: CD74, MIF, fusion proteins, solubility enhancers.

Running head: **Production of CD74 fused to solubility enhancing peptides**

Abbreviations

| | |
|----------|--|
| BSA | bovine serum albumin |
| CD74 | cluster of differentiation 74 |
| CLIP | class II-associated Ii peptide |
| ELISA | enzyme-linked immunosorbent assay |
| Fh8 | <i>Fasciola hepatica</i> 8-kDa antigen |
| Ii | invariant chain |
| MBP | maltose binding protein |
| MHCII | major histocompatibility complex class II molecules |
| MIF | macrophage migration inhibitory factor |
| PBS | phosphate-buffered saline |
| PCR | polymerase chain reaction |
| SDS PAGE | sodium dodecyl sulphate polyacrylamide gel electrophoresis |
| ITC | isothermal titration calorimetry |

Introduction

CD74 (Cluster of Differentiation 74), also referred to as HLA class II histocompatibility antigen gamma chain or HLA-DR antigen-associated invariant chain Ii, is a non-polymorphic type II transmembrane glycoprotein that has been demonstrated to perform a variety of cellular functions. It was initially identified in complex with major histocompatibility complex class II (MHCII) molecules and soon recognized for its role in antigen presentation via its involvement in assembly and subcellular trafficking of the MHCII complex [1]. The four isoforms of human CD74 differ in activity and cellular expression [2][3]. Due to an arginine motif in their N-terminal extension, isoforms p35 and p43 are retained in the endoplasmic reticulum (ER) except when they form a complex with MHCII molecules, in which this retention motif is masked so that the complex can traffic to post-ER compartments. Typically, the luminal domain of CD74 undergoes progressive proteolytic degradation in the endosomal/lysosomal system, finally leaving a fragment, the small class-II-associated invariant chain peptide (CLIP), attached to the MHC class II molecule. In contrast to p35 and p45, isoforms p33 and p41 do not have the ER retention signal allowing these isoforms to traffic in non-MHCII expressing cells [3].

In addition to its role in subcellular trafficking, a small portion of CD74 functions as a cellular receptor for the immune regulatory cytokine macrophage migration inhibitory factor (MIF). Although MIF can also bind to G-protein coupled receptors CXCR2, CXCR4 and CXCR7, the CD74-mediated signaling is recognized to play an important role in many diseases connected to inflammation, as well as cell proliferation and differentiation [4][5][6]. Recently, serum levels of not only MIF but also the soluble, circulating version of CD74 were reported to be related to liver and respiratory diseases [7][8]. Taken together, the MIF-CD74 interaction and the related signaling pathway have become attractive targets for novel therapies, as also illustrated by the humanized monoclonal anti-CD74 antibody milatuzumab that recently received orphan drug designation from the Food and Drug Administration in the USA for the treatment of multiple myeloma and chronic lymphocytic leukemia [9]. Excellent descriptions of the biological and structural aspects of CD74 can be found in two recent reviews [2] [10].

In the light of CD74's fate in the endosomal/lysosomal system, it may not be surprising that the study of the binding of MIF to CD74 is hampered by the partially unstable structure of CD74; only the trimerisation domain within the extracellular moiety appears to have a stable structure [11]. In addition, the production yield of the extracellular moiety of CD74 in bacterial cells is not very high [12]. The application of fusion technology via the use of affinity fusion tags, in particular solubility enhancing peptides, is frequently used to improve the yield of active, pure protein [13][14][15]. We have tested two affinity tags: the well-documented maltose-binding protein (MBP) and the recently reported small EF-hand protein Fh8 from the parasitic trematode *Fasciola hepatica*. MBP is a large (43kDa), highly soluble protein of *E. coli* that acts as a solubility enhancer tag [16]. For purification, MBP fusion proteins can bind to immobilized amylose resins and be eluted using maltose [17]. Similar to MBP, the small (8 kDa) protein Fh8 combines solubility enhancing properties to the possibility of affinity chromatography [18][19][20].

In this study we made use of the MBP and Fh8 fusion partners to obtain a high yield of soluble CD74 and characterized the purified fusion proteins for binding to MIF. In addition to the fused proteins, we also tested the cleaved products for their binding activity. The results

allowed us to conclude that the extracellular moiety of CD74 between the transmembrane region and the membrane-distal trimerisation domain, in particular amino acids 113-125, is involved in binding of MIF.

Materials and methods

Procedures for restriction enzyme digestions, ligation, transformation, and other standard molecular biology manipulations were performed as described by Sambrook *et al.* [21]. The PCR was carried out in a DNA thermal cycler model GS-1 (Biolegio, The Netherlands). DNA sequencing was performed by Macrogen, Korea. Proteins were analyzed by gel electrophoresis using 10% sodium dodecyl sulphate polyacrylamide gels (SDS-PAGE; Invitrogen, The Netherlands). The gels were stained with InstantBlue protein stain (Expedeon, UK). Protein markers used for SDS-PAGE were PageRuler Prestained Protein Ladder marker (Thermo Scientific, The Netherlands) or SeeBlue Plus2 Prestained marker (Invitrogen, The Netherlands).

Protein concentrations were determined by the Pierce[™] Coomassie Protein Assay (ThermoFischer Scientific, The Netherlands) using bovine serum albumin as a reference. Molar concentrations of MIF and CD74 proteins refer to the concentrations of their subunits.

Molecular weight analysis of purified proteins or proteins extracted from SDS-PAGE gels were performed by electrospray ionization-mass spectrometry using a Sciex API 3000 triple quadrupole mass spectrometer (AB Sciex, Canada), housed in the Mass Spectrometry Facility at the University of Groningen.

Plasmids and bacterial strains

The plasmid and bacterial strain used for MIF production in this study was pET20b(+) (Addgene, UK) and *E.coli* BL21 (DE3), respectively [22]. The plasmid and bacterial strains used for CD74 production were pET20b(+) and *Rosetta-gami* 2(DE3) (Novagen, Germany) for MBP the fusion proteins; and pET14b (Addgene, UK) and *E. coli* BL21 star (DE3) pRARE2 (Thermo Fisher Scientific, The Netherlands) for the Fh8 fusion proteins.

DNA manipulations

(i) **Construction of pET20b-MBP-sCD74 expression vector.** Plasmid pCR T7/CT TOPO encoding the extracellular domain of human CD74 with a C-terminal His-tag was a kind gift from Prof. Richard Bucala [4].

The MBP-sCD74 fusion construct was generated by the overlap extension PCR method. The first DNA fragment, containing the MBP gene and the sequence encoding the factor Xa cleavage site, was amplified by PCR using pMAL-c2X vector as a template and a pair of primers: MBP-EXT-Fw (5'-CAG CGA **CAT ATG** AAA ATC GAA GAA GGT AAA CTG GTA ATC-3'; *Nde*I site in bold) and MBP-FUS-Rv (5'-ACG ACC TTC GAT GAA TTC TGA AAT CCT TCC CTC GAT CCC GAG GTT-3'; nucleotide sequence encoding the factor Xa cleavage site is underlined). The second fragment, containing the sCD74 gene was

amplified using pET20b (sCD74) as a template. Plasmid pET20b-sCD74 was made as follows: the CD74 gene was amplified (primers: CD74-Fw: 5'-CAG CGA **CAT ATG CAG GGC CGG CTG GAC AAA CTG ACA GTC ACC**-3', *NdeI* site in bold; and CD74-Rv: 5'-CTG ATG GAT **CTC GAG** CAT GGG GAC TGG GCC CAG ATC CTG CTT-3', *XhoI* site in bold) and, after *NdeI/XhoI*-digestion, ligated into the pET20b vector. The sCD74 gene fragment was amplified from this plasmid using the following primers: MBP-FUS-Fw (5'-AAC CTC GGG ATC GAG GGA AGG ATT TCA GAA TTC ATC GAA GGT CGT CAG GGC CGG CTG GAC AAA CTG ACA GTC ACC TC-3'; nucleotide sequences for factor Xa cleavage site underlined) and CD74-Rv. The two fragments generated in the first round of PCR were fused in the second round using MBP-EXT-Fw and CD74-Rv primers. After digestion with *NdeI* and *XhoI* and purification, this fragment was ligated into the pET20b vector cleaved with the same restriction enzymes. The newly constructed expression vector was denoted pET20b-MBP-sCD74 and its fidelity was confirmed by DNA sequencing.

(ii) Construction of pCoBo-Fh8-sCD74 and pCoBo-Fh8-ssCD74 expression vectors. For production of Fh8-fused proteins, a modified pET15b vector was created that contains two multiple cloning sites separated by a 3C cleavage sequence in the following manner: (1) The *HindIII* site in pET15b was removed by mutagenesis; (2) oligonucleotides were designed with restriction sites *AgeI* and *KpnI* followed by a DNA stretch encoding the rhinovirus 3C proteolytic site (LEVLFQ/GP) and with a *NcoI* sequence on each end of the oligonucleotides, allowing cloning into the *NcoI* site of pET15b. The oligos were designed in such a manner that the “upstream” *NcoI* site closest to the T7 promoter would be lost. The proper orientation of this insert in the modified plasmid was checked by restriction analysis and sequencing; (3) The DNA encoding Fh8 was amplified from plasmid pD454-Fh8 (DNA2.0 Inc., U.S.A.) using the following primers carrying *AgeI* and *KpnI* restriction sites (in bold), respectively: Fh8AQUAFwd (5'-TTA AGA AGG AGA TAT ACC ATG CAA **ACC GGT** ATG CCG AGC GTT CAA GAA G-3') and Fh8AQUARev (5'-TTG AAA AAG CAC TTC AAG ACC **TCC GGT ACC** AGA TGT GCC GCT GCT CAG-3'). The DNA fragment was cloned into the modified pET15b vector cleaved with *AgeI* and *KpnI* using AQUA cloning [23]; (4) Oligonucleotides were designed to insert a new multiple cloning site comprising restriction sites *BamHI*, *HindIII*, *NdeI*, *SmaI*, *XhoI*, *XmaI*, with an upstream *NcoI* site and a dysfunctional *BamHI* site downstream. The hybridised oligos were ligated in the plasmid cleaved with *NcoI* and *BamHI*. This plasmid was named pCoBo-Fh8.

The CD74 gene on the pET20b-MBP-sCD74 plasmid was amplified using the following primers: CD74-Fwd (5'-GCA TCA GGA TCC ATT GGA GCA AAT **AAG CTT** CGG CTG GAC AAA CTG AC-3') and CD74-Rev (5'-TTG TTA GCA GCC GGA TCG TCA TTA **CCC GGG** GG ATC TCA GTG GTG GTG-3') for Fh8-sCD74; and CD74-Fwd (5'-GCA TCA GGA TCC ATT GGA GCA AAT **AAG CTT** CTG CTG ATG CAG GCG-3') and CD74-Rev (5'-TTG TTA GCA GCC GGA TCG TCA TTA **CCC GGG** GG ATC TCA GTG GTG GTG-3') for Fh8-ssCD74, carrying *HindIII* and *SmaI* restriction sites (bold). After digestion, the DNA fragment was ligated into the pCoBo-Fh8 vector cleaved with *HindIII* and *SmaI*, resulting in pCoBo-Fh8-sCD74 and pCoBo-Fh8-ssCD74, respectively. The inserts of all constructs were checked by DNA sequencing.

Protein production and purification

(i) Production and purification of CD74 fusion proteins. The pET20b-MBP-sCD74 and pCoBo-Fh8-sCD74 were transformed into *Rossetta-gami 2* (DE3) and BL21 Star (DE3) +pRARE2 strain, respectively. For protein production, overnight pre-cultures were used to

inoculate 1 L 2YT medium in a 5 L Erlenmeyer flask. Cultures were then grown until $OD_{600} \sim 0.5$. Isopropyl β -thiogalactopyranoside was added to a final concentration of 50 μ M and the cultures were incubated overnight at 20 °C. Cells were harvested by centrifugation (3500 \times g, 15 min, 4 °C), washed with 0.9 % NaCl and the cell pellet stored at -20 °C until further use. In a typical purification experiment, 10 g cell pellets from a 1 L culture were thawed and suspended in 15 mL of lysis buffer (50 mM Tris-HCl, 10% glycerol, pH 7.4) supplemented with 1 tablet protease inhibitor (Roche, The Netherlands), 19 mg EDTA and 19 mg EGTA. Cells were disrupted by sonication for 6 \times 30 s while cooled in ice-water (with 90 s rest in between each cycle) at a 50% duty cycle and 240 W output using a Branson sonifier model 450 (Branson Ultrasonics Corporation, U.S.A.), after which cell debris was removed by centrifugation (34,000 \times g, 60 min, 4 °C). The cell free extract (supernatant) was incubated overnight at 4 °C with 5 mL cComplete HisTrap purification resin (Roche Life Science, The Netherlands), pre-equilibrated with lysis buffer. The non-bound proteins were removed as flow through by gravity flow. The column was then washed with 50 mL lysis buffer followed by 12 mL HT elution buffer (50 mM Tris-HCl, 500 mM imidazole, 10% glycerol, pH 7.4). Fractions were analyzed by SDS PAGE and those containing CD74 fusion proteins pooled.

HisTrap-purified MBP-fused CD74 proteins was applied to a gravity column containing 5 mL MBPTrap resin, pre-equilibrated with MT buffer (50 mM Tris-HCl, 10% glycerol, pH 7.4). After an overnight incubation at 4 °C while mixing on a rotor, the non-bound proteins were removed from the column with 50 mL of MT buffer. Bound protein was eluted with 3.5 mL MT elution buffer (50 mM Tris-HCl, 10 mM maltose, 10% glycerol, pH 7.4). Fractions were analyzed by SDS PAGE, those containing CD74 fusion proteins were pooled, aliquoted, snapfrozen and stored in aliquots at -80 °C.

Fh8-fused CD74 proteins could be further purified by a 5 mL octyl sepharose column (GE Healthcare, The Netherlands) at 10 °C as described [12]. In short, the protein was dialysed against OS buffer (50 mM Tris-HCl, 150 mM NaCl, 5 mM $CaCl_2$, 10% glycerol, pH 7.6) and loaded on a 5-mL octyl sepharose column (GE Healthcare, The Netherlands), pre-equilibrated with OS buffer. After washing with low $CaCl_2$ -buffer (25 mM Tris-HCl, 75 mM NaCl, 2.5 mM $CaCl_2$, 10% glycerol, pH 7.6), the protein was eluted with 50 mM Tris, 5 mM EDTA, 10% glycerol, pH 7.6. Fractions were analyzed by SDS PAGE, those containing Fh8-fusion proteins were pooled, aliquoted, snapfrozen and stored in aliquots at -80 °C.

(ii) Factor Xa cleavage of MBP-sCD74. The cleavage of the MBP-sCD74 fusion protein was performed in 50 mM Tris-HCl, 10% glycerol supplemented with 50 mM NaCl and 2 mM $CaCl_2$ at pH 7.4 by factor Xa protease (NEB, The Netherlands) with a mass/volume (μ g/ μ L) ratio MBP-sCD74:factor Xa of 25:1, 3 hours incubation period at 4 °C. The cleaved product was purified using cComplete His-Trap purification resin. Fractions were analyzed by SDS PAGE, those containing sCD74 were pooled, aliquoted, snapfrozen and stored in aliquots at -80 °C.

(iii) 3C cleavage of Fh8-ssCD74. The cleavage of the Fh8-ssCD74 fusion protein was performed in 50 mM Tris-HCl, 10% glycerol supplemented with 150 mM NaCl at pH 7.4 by 3C PreScission protease (GE Healthcare, The Netherlands) with a mass/volume (μ g/ μ L) ratio Fh8-ssCD74:3C of 100:1, 1 hour at 4 °C. The cleaved product was purified using octyl sepharose resin (GE Healthcare, The Netherlands) followed by cComplete His-Trap purification resin, as described above. Fractions were analyzed by SDS PAGE, those containing ssCD74 were pooled, aliquoted, snapfrozen and stored in aliquots at -80 °C. Protein sssCD74, produced by overnight incubation of Fh8-ssCD74 with 3C Precision protease at 4 °C, was purified using cComplete HisTrap resin.

(iv) **Peptides MBP and Fh8.** Proteins MBP was purchased from ProSpec-Tany TechnoGene Ltd (Germany). Fh8 was produced with pCoBo-Fh8 and purified using octyl sepharose resin.

(v) **Production and purification of MIF.** MIF was produced in BL21(DE3) in a similar manner as MBP-sCD74. After harvesting, cells were resuspended in lysis buffer supplemented with 1 tablet protease inhibitor (Roche, The Netherlands). Cell free extract was obtained as described earlier for MBP-sCD74 and incubated overnight at 4 °C with 5 mL cComplete His-Trap purification resin (Roche, The Netherlands), which had previously been equilibrated with the lysis buffer. The non-bound proteins were removed as flow through by gravity flow. The column was washed with 50 mL lysis buffer followed by 12 mL elution buffer (50 mM Tris-HCl, 500 mM imidazole, 10% glycerol, pH 7.4). Fractions were analyzed by SDS PAGE and those containing MIF were pooled, aliquoted, snap-frozen and stored at -80 °C.

Analysis of proteins using size exclusion chromatography

MIF and CD74 proteins were analysed separately on an analytical size exclusion column. 20 µL of a 1 mg/mL protein solution was injected and run at 0.2 mL/min on a 3 ml Superdex200 5/150 column (GE Healthcare), equilibrated with PBS, pH 7.4, at 10 °C. To calibrate the column, the elution volumes of five marker proteins (GE Healthcare) were determined under identical conditions: thyroglobulin (669 kDa), ferritin (440 kDa), aldolase (158 kDa), conalbumin (75 kDa), and ovalbumin (43 kDa).

Binding assays

Enzyme-linked immunosorbent assay (ELISA)

The sCD74 proteins were characterised for MIF binding in an ELISA test. Wells in 96-well plates were coated with 100 µL of 300 nM MIF in phosphate-buffered saline (PBS) [400 ng/well]. After washing with 200 µL buffer PBS+Tween 0.05% and blocking with commercial blocker (Rockland, The Netherlands), 100 µL of 500 nM sCD74 was added, and the system was incubated for 30 min at room temperature. After the wells were washed and blocked, mouse anti-MBP mAb (SigmaAldrich, The Netherlands) or rabbit anti-CD74 pAb (Sinobiological, The Netherlands) was added. The bound complexes were detected after washing by the addition of goat anti-mouse horseradish peroxidase conjugate (Thermo Fisher Scientific, The Netherlands) or goat anti-rabbit horseradish peroxidase conjugate (Life Technologies, The Netherlands), and tetra methylbenzidine (Thermo Fisher Scientific, The Netherlands) as its substrate. After ~10 min the reaction was stopped by the addition of 1M H₂SO₄ and the absorbance at 450 nm measured. The specificity of binding was confirmed by using 100 µL of 500 nM MBP in PBS, and 100 µL of 500 nM Fh8 in PBS as controls. Each experiment was done in triplicate and repeated at least two times.

A dose-dependent ELISA was performed with sCD74 concentration ranging from 3 to 3200 nM (for MBP-sCD74) and 12 to 3200 nM (for Fh8-ssCD74). The corrected absorbance at 450 nm was then plotted against logarithm of concentration to find the dissociation constant of the binding.

Isothermal Titration Calorimetry (ITC)

Binding of MIF to CD74 was measured by ITC model ITC200 (Malvern, UK) at 25 °C, 1000 rpm stirring speed, 120 seconds spacing between each injection. The cell was filled with 200 μ L of 40-85 μ M MBP-sCD74 in PBS and titrated with 20 consecutive injections of 2 μ L 70-220 μ M MIF in PBS. A cell filled with PBS only titrated with MIF and a cell filled with fusion protein titrated with PBS only were used as control.

Results and Discussion

Even though MIF was one of the first cytokines to have been described, many details of its signaling activities still have to be elucidated. Nevertheless, the involvement of receptor CD74 has been proven in many MIF-related diseases and this receptor has been recognised as a major pharmaceutical target. The interaction between MIF and CD74 was *in vitro* demonstrated to be located in the extracellular moiety of CD74 [4][24]. However, the unstable and protease-prone character of the extracellular moiety of CD74 has hampered further characterisation. Several attempts to obtain a good production of the extracellular moiety of CD74 with a C-terminal His-tag in bacteria resulted in low yields of soluble protein [12]. As a consequence, we have tried to tackle this problem by fusing CD74 to solubility-enhancing peptides. Two different solubility enhancing peptides were used: the large, but well characterised MBP protein [14] and the recently reported small protein Fh8 [16][17][18]. **Figure 1** presents a schematic overview of the fusion proteins encoded by the constructs that were made, and their corresponding amino acid sequences.

Production and purification of CD74 proteins

The fragments of the human CD74 gene as cloned into the expression vectors were not codon-optimized for bacterial expression. Therefore, we used *E.coli* strains that were transformed with the plasmid pRARE2 supplying tRNAs for 7 rare codons (AGA, AGG, AUA, CUA, GGA, CCC, and CGG), e.g. the strains *Rossetta-gami 2* (DE3) and BL21 Star (DE3) + pRARE2. This allowed high production yields of soluble MBP-sCD74, Fh8-sCD74 and Fh8-ssCD74 (**Figure 2**).

Fusion protein MBP-sCD74 was successfully purified by affinity chromatography using a HisTrap column followed by a MBP-Trap column. Mass spectrometric analysis of the major band running just below the 62 kDa marker protein (**Figure 3**, lane 3) gave a mass of 62.326 kDa which corresponds to the calculated MW of 62.319 kDa. MS analysis of the tryptic digestion of the protein confirmed the identity of MBP-sCD74 by >90 % coverage. About ~60 mg of purified MBP-sCD74 was obtained from one liter of culture. Mass analysis of a contaminating protein running above the 14 kDa marker protein (**Figure 3**, lane 3) showed this to be a 14.711 kDa peptide, corresponding to a degradation product with a proteolytic cleavage between residues Pro112 and Leu113 of CD74. This deviates from previously observed cleavage sites in this region [25][26], a difference that is likely to be related to differences in *E. coli* strains and growth conditions that were used, and /or to the N- or C-terminally located His-tag leading to purification of different fragments. The proteolytic sensitivity is supported by the NMR study of fragment 133-208 of CD74, which showed that amino acids directly flanking the trimerisation domain are disordered [27]. In line with this, the CLIP region (residues 97-119) appears as a linear peptide without secondary structure in complex with MHCII molecules [28][29][30][31].

The large size of MBP (42 kDa) made us decide to also construct a fusion of sCD74 with the much smaller Fh8 protein, an EF-hand protein of 8 kDa that shows calcium-dependent binding to hydrophobic resins. The Fh8-sCD74 fusion protein was first purified by affinity chromatography on a HisTrap column. Similar to MBP-sCD74, purification of Fh8-sCD74 on the cOmplete HisTrap column resulted in an approximately 90% pure protein with an experimentally determined mass of 29.604 kDa, corresponding to the calculated mass of 29.605 kDa. The yield of Fh8-sCD74 was 30 mg per liter culture. Mass analysis of the contaminant protein running above the 14 kDa marker protein in the SDS-PAGE gel (**Figure 3**, lane 2) demonstrated this protein to have a mass of 14.711 kDa, similar to the contamination found in the MBP-sCD74 protein batch. Unfortunately, the octyl sepharose column did not improve the purity of the fusion protein. The difficulty to remove degradation products from fusion products are most likely due to the multimeric character of CD74: cleavage in loop regions does not necessarily affect trimer formation of CD74-derived proteins nor their chromatographic behaviour.

In an attempt to create a more protease-stable fragment of sCD74, a plasmid encoding fusion protein Fh8-ssCD74 (CD74 residues 113-232) was constructed (**Figure 1**). Production of this protein and purification on a cOmplete HisTrap column (**Figure 3**, lane 1) resulted in the high yield of 75 mg of ~95% pure protein per liter of culture with an experimentally determined mass of 25.461 kDa, corresponding to the calculated mass of 25.462 kDa. As anticipated, the previously observed contaminant of 14.711 kDa was not found in this protein batch.

In order to obtain the non-fused sCD74, fusion protein MBP-sCD74 was cleaved with factor Xa, followed by purification on a HisTrap column. This resulted in a mixture of sCD74 and lower molecular weight products (**Figure 3**, lane 5). Apparently, the MBP-sCD74 fusion protein is prone to cleavage with factor Xa at additional sites. Attempts to improve the purity of sCD74 by size exclusion and ion exchange chromatography were unsuccessful.

Similarly, 3C-mediated cleavage of Fh8-ssCD74 and subsequent purification of ssCD74 also resulted in a mixture of proteins of slightly smaller mass (results not shown). Also here, chromatography attempts to recover ssCD74 using HisTrap as a highly purified protein were not successful. Further experimentation indicated that a stable cleavage product of ssCD74, denoted as sssCD74, was obtained after overnight incubation at 4 °C with 3C protease. Mass spectrometry analysis demonstrated that the molecular weight of this product was 13.343 kDa, corresponding to residues 126-232 with C-terminal His-tag, thus lacking almost the whole region up to the membrane-distal trimerisation domain of CD74 (**Figure 1**). This fragment could be highly purified with a cOmplete HisTrap column (**Figure 3**, lane 6). Noteworthy, fragment sssCD74 is comparable to the 18 kDa proteolytic fragment K3, that retains the ability to bind to MHCII molecules, and, like sssCD74, starts at residue Gly126 but has a C-terminal truncation [32].

When analyzed on an analytical size exclusion column, the fusion proteins MBP-sCD74, Fh8-sCD74 and Fh8-ssCD74 eluted earlier than expected (**Figure 4**). Although expected to run as trimers with molecular weights 186.9, 88.8, and 77.5 kDa, respectively, they eluted between the reference proteins ferritin (MW 440 kDa) and aldolase (158 kDa). At first impression, this seems to indicate that the fusion proteins form hexameric instead of trimeric structures. However, since fusion partners MBP and Fh8 are considered to be stable monomers, and since the elution volumes of cleaved products sCD74 and sssCD74 correspond to the expected elution volumes of their trimeric versions (60.9 and 39.9 kDa, respectively), this behaviour is

more likely to be a consequence of increased hydrodynamic shapes of the trimeric fusion proteins. Such behaviour is not unexpected for fusion proteins that consist of two well-defined domains separated by an intrinsically disordered moiety. Our results suggest that all CD74 proteins used in this study are mostly present in a homotrimeric form. However, the chromatograms of the three fusion proteins show more than one peak indicating some heterogeneity. Fh8-sCD74 shows two major peaks which are not easily explained. MBP-sCD74 and Fh8-sCD74 show a small peak at c. 40 kDa, which can be interpreted as the trimer of the 14.711 kDa contamination.

As expected, the elution volume of MIF fits to its trimeric form (40.3 kDa; **Figure 4**).

MIF binding capacities of CD74 proteins

The MIF binding capacities of the different CD74 proteins were assessed by ELISA. As depicted in **Figure 5A** and **B**, all fusion proteins of CD74 were able to bind to this cytokine. The lack of MIF binding to the MBP and Fh8 polypeptides demonstrated that the interactions of the CD74 fusion proteins with MIF are a consequence of the presence of CD74 and not of the fusion partners. Interestingly, at a concentration of 500 nM, fusion protein Fh8-ssCD74 gave a lower MIF-binding response than Fh8-sCD74 (**Figure 5B**) indicating that deletion of residues 77-112 of CD74 only partially affects the binding to MIF. The binding capacity of 500 nM non-fused sCD74 itself is also shown in **Figure 5C**. Deletion of residues 77-125 in the luminal moiety up to the membrane-distal trimerisation domain resulted in a complete loss of MIF binding capacity as is demonstrated by the lack of binding of 500 nM purified protein sssCD74 (**Figure 5C**). This is not due to a loss of structural stability since both sCD74 and sssCD74 behave as trimeric proteins during size exclusion chromatography (**Figure 4**). These results thus strongly suggest that the MIF-binding region lies N-terminal to the membrane-distal trimerisation domain of CD74.

These biochemical results differ from the results of a docking experiment in which amino acid sequences YGNMT and RHSLE within the trimerisation domain were predicted to be involved in the binding to MIF [33]. The docking experiment – as it is depending on three-dimensional structures - was performed with the crystal structures of MIF (PDB ID: 1MIF) and the membrane-distal trimerisation domain of CD74 (PDB ID: 1IIE), hence excluding the disordered region N-terminal to the trimerisation domain. Our results, especially the lack of interaction of sssCD74 with MIF in our ELISA assay (**Figure 5C**), indicate that the membrane-distal CD74 trimerisation domain is not or only weakly involved in the interaction with MIF, and is not sufficient for a high affinity interaction.

In order to get further insight in the formation of a complex between MIF and CD74, we performed a dose-dependent ELISA with MBP-sCD74 and Fh8-ssCD74 (**Figure 6**). Whereas the binding isotherm of MBP-sCD74 leads to an EC₅₀-value of approximately 110 nM, Fh8-ssCD74 leads to a 2.5-fold higher value of approximately 280 nM, suggesting that removal of residues 77-112 of CD74 is affecting but not destructing the interaction with MIF. Together with the lack of MIF-binding by sssCD74 (i.e. amino acids 126-232), these results indicate that CD74 amino acids 113-125 are of primary importance for the interaction with MIF, and that the amino acids N-terminal to this region add to the binding ability. ITC binding kinetics measurements confirmed that MIF binds to MBP-sCD74 (**Figure 7**). Complex formation is an exothermic reaction with a reaction enthalpy (ΔH) of $-(2.5 \pm 0.5) \cdot 10^6$ cal/mol. This low enthalpy value made obtaining solid data of ITC experimentation rather difficult. The

apparent dissociation constant (K_D) was $1.3 \pm 0.1 \mu\text{M}$. This affinity is lower than the EC_{50} -value obtained with ELISA.

Earlier SPR measurements of the interaction between MIF and sCD74 have resulted in significantly higher reported affinities of 0.23 or 9 nM, depending on the experimental configuration [4]. We note, however, that the lack of details in this SPR study does not allow a direct comparison. Interestingly, the same study also shows a sandwich ELISA that seems to point at an EC_{50} value in the submicromolar range of sCD74, which is comparable to our ELISA results. The affinity measurements thus show considerable variety, which may be caused by different complex formation between these multimeric proteins under different experimental conditions. As Leng et al [4] pointed out: based on the serum concentration of MIF, one would expect a nanomolar range affinity for its receptor. In that light it should be noted that the *in vitro* results have been obtained with bacterially produced proteins. The native proteins, with possible post-translational modifications on MIF and CD74 (e.g. oxidation and glycosylation; [34]) may have different affinities. In addition, the transmembrane domain of CD74 is also able to trimerize [35][36] and thus may bring extra stability and raise the affinity for MIF.

Interestingly, the molar binding ratio in our ITC experiment was found to be 0.29 ± 0.03 . Assuming all MBP-sCD74 and MIF molecules to be active, this molar ratio indicates that a complex of a trimeric MIF with 3 trimers of MBP-sCD74 is formed. This suggests that MIF initiates signaling by clustering the trimeric CD74 receptor into a larger network that is needed to overcome the threshold for initiation of the signaling cascade.

Conclusions

Our research demonstrated that the luminal portion of CD74 can be produced at high yields in a bacterial expression system when fused to the solubility enhancing proteins MBP and Fh8. The purified fusion proteins were demonstrated to bind to MIF. The extracellular region from the transmembrane domain up to the membrane-distal trimerisation domain of CD74 appears to be essential for this interaction, with amino acids 113-125 being an important region, as demonstrated by the binding assays with different constructs.

The successful production of functional CD74 in high quantities, whether as a fusion protein or as cleaved product, is the first step in further characterisation of its structural features and of the elucidation of the binding mechanism of mammalian MIF and MIF homologues to this receptor. Moreover, it will stimulate our search for clinically relevant inhibitors of the MIF-CD74 interaction.

Acknowledgements

We thank Prof. Richard Bucala, Yale/New haven Hospital, for kindly providing the human CD74 gene. We acknowledge Jan Ytzen van de Meer, Bas Vriezelaar, Angela Asselman, Ykelien Boersma, Ronald van Merkerk, Laura Sampredo and Gea Schuurman-Wolters for assistance and support given during our research. This work was supported by a grant 94.18/E4.4/2014 from Directorate General of Higher Education Indonesia (DIKTI) in collaboration with the University of Surabaya (Ubaya), Indonesia and the University of Groningen (RuG), The Netherlands.

Author contribution statement

FJD and GJP conceived and supervised the project, TK and AAW with the assistance of RHC designed the experiments. TK and AAW performed the experiments. TK with the assistance of RHC analyzed and interpreted the data. TK and RHC wrote the paper. GJP and FJD gave input for revisions of the manuscript.

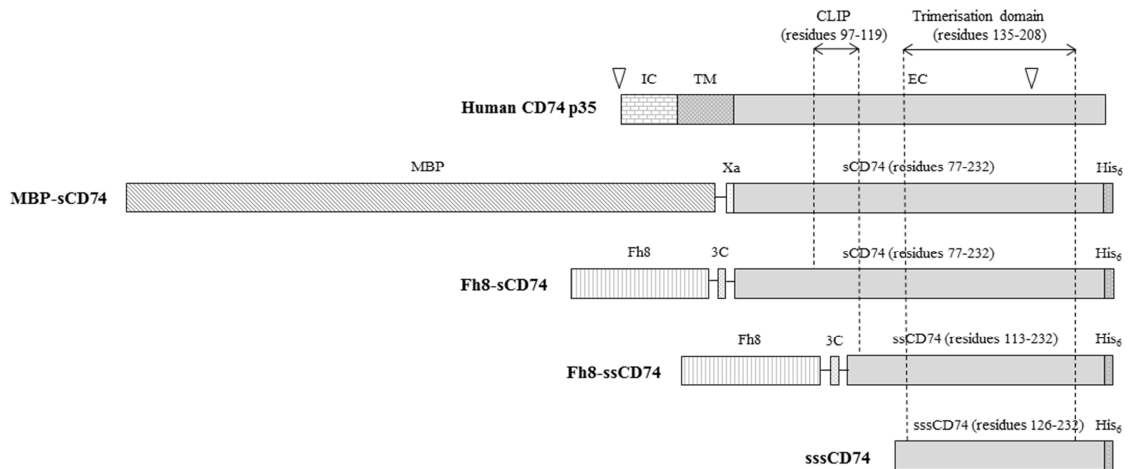
References

- [1] F. Borghese, F. IL Clanchy, CD74: an emerging opportunity as a therapeutic target in cancer and autoimmune disease, *Expert Opin. Ther. Targets*. 15 (2011) 237–251. doi:10.1517/14728222.2011.550879.
- [2] B. Schroder, The multifaceted roles of the invariant chain CD74 - More than just a chaperone, *Biochim. Biophys. Acta - Mol. Cell Res.* 1863 (2016) 1269–1281. doi:10.1016/j.bbamcr.2016.03.026.
- [3] M. Strubin, C. Berte, B. Mach, Alternative splicing and alternative initiation of translation explain the four forms of the Ia antigen-associated invariant chain, *EMBO J.* 5 (1986) 3483–8.
- [4] L. Leng, C.N. Metz, Y. Fang, J. Xu, S. Donnelly, J. Baugh, T. Delohery, Y. Chen, R.A. Mitchell, R. Bucala, MIF Signal Transduction Initiated by Binding to CD74, *J. Exp. Med.* 197 (2003) 1467–1476. doi:10.1084/jem.20030286.
- [5] K.L. Meyer-Siegler, K. a Iczkowski, L. Leng, R. Bucala, P.L. Vera, Inhibition of macrophage migration inhibitory factor or its receptor (CD74) attenuates growth and invasion of DU-145 prostate cancer cells, *J. Immunol.* 177 (2006) 8730–8739. doi:177/12/8730.
- [6] H. Su, N. Na, X. Zhang, Y. Zhao, The biological function and significance of CD74 in immune diseases, *Inflamm. Res.* 66 (2017) 209–216. doi:10.1007/s00011-016-0995-1.
- [7] D.N. Assis, L. Leng, X. Du, C.K. Zhang, G. Grieb, M. Merk, A.B. Garcia, C. McCrann, J. Chapiro, A. Meinhardt, Y. Mizue, D.J. Nikolic-Paterson, J. Bernhagen, M.M. Kaplan, H. Zhao, J.L. Boyer, R. Bucala, The Role of Macrophage Migration Inhibitory Factor in Autoimmune Liver Disease, *Hepatology.* 59 (2014) 580–591. doi:10.1002/hep.26664.
- [8] G. Wu, Y. Sun, K. Wang, Z. Chen, X. Wang, F. Chang, T. Li, Relationship between elevated soluble CD74 and severity of experimental and clinical ALI / ARDS, *Nat. Publ. Gr.* (2016) 1–20. doi:10.1038/srep30067.
- [9] M. Podhorecka, J. Markowicz, A. Szymczyk, J. Pawlowski, Target therapy in hematological malignances: new monoclonal antibodies, *Int. Sch. Res. Not.* 2014 (2014) 1–16. doi:10.1155/2014/701493.
- [10] R. Lindner, Invariant Chain Complexes and Clusters as Platforms for MIF Signaling, *Cells.* 6 (2017) 6. doi:10.3390/cells6010006.
- [11] G. Pantouris, M.A. Syed, C. Fan, D. Rajasekaran, T.Y. Cho, E.M. Rosenberg, R. Bucala, V. Bhandari, E.J. Lolis, E.J. Lolis, An Analysis of MIF Structural Features that

- Control Functional Activation of CD74, *Chem. Biol.* 22 (2015) 1197–205.
doi:10.1016/j.chembiol.2015.08.006.
- [12] A.A. Wasiel, Macrophage Migration Inhibitory Factor Cell Surface Receptor, Enzymatic Activities and Evolutionary History of A Multifunctional Cytokine, PhD thesis, University of Groningen, The Netherlands (2013), ISBN 978-90-367-6152-9.
- [13] D. Esposito, D.K. Chatterjee, Enhancement of soluble protein expression through the use of fusion tags, *Curr. Opin. Biotechnol.* 17 (2006) 353–358.
doi:10.1016/j.copbio.2006.06.003.
- [14] R.B. Kapust, D.S. Waugh, Escherichia coli maltose-binding protein is uncommonly effective at promoting the solubility of polypeptides to which it is fused, *Protein Sci.* 8 (1999) 1668–1674. doi:10.1110/ps.8.8.1668.
- [15] S. Costa, A. Almeida, A. Castro, L. Domingues, Fusion tags for protein solubility, purification, and immunogenicity in Escherichia coli: The novel Fh8 system, *Front. Microbiol.* 5 (2014) 1–20. doi:10.3389/fmicb.2014.00063.
- [16] J.D. Fox, R.B. Kapust, D.S. Waugh, Single amino acid substitutions on the surface of Escherichia coli maltose-binding protein can have a profound impact on the solubility of fusion proteins, *Protein Sci.* 10 (2001) 622–630. doi:10.1110/ps.45201.
- [17] K.D. Pryor, B. Leiting, High-Level Expression of Soluble Protein in Escherichia coli Using a His6-Tag and Maltose-Binding-Protein Double-Affinity Fusion System, *Protein Expr. Purif.* 10 (1997) 309–319. doi:10.1006/pep.1997.0759.
- [18] S.J. Costa, A. Almeida, A. Castro, L. Domingues, H. Besir, The novel Fh8 and H fusion partners for soluble protein expression in Escherichia coli: A comparison with the traditional gene fusion technology, *Appl. Microbiol. Biotechnol.* 97 (2013) 6779–6791. doi:10.1007/s00253-012-4559-1.
- [19] S.J. Costa, E. Coelho, L. Franco, A. Almeida, A. Castro, L. Domingues, The Fh8 tag: A fusion partner for simple and cost-effective protein purification in Escherichia coli, *Protein Expr. Purif.* 92 (2013) 163–170. doi:10.1016/j.pep.2013.09.013.
- [20] H. Fraga, T.Q. Faria, F. Pinto, A. Almeida, R.M.M. Brito, A.M. Damas, FH8 - A small EF-hand protein from Fasciola hepatica, *FEBS J.* 277 (2010) 5072–5085.
doi:10.1111/j.1742-4658.2010.07912.x.
- [21] J. Sambrook, E.F. Fritsch, T. Maniatis, *Molecular Cloning: A Laboratory Manual*, 2nd ed., Cold Spring Harbor Laboratory Press, Cold Spring Harbor, NY (1989).
- [22] A.A. Wasiel, H.J. Rozeboom, D. Hauke, B.J. Baas, E. Zandvoort, W.J. Quax, A.M. Thunnissen, G.J. Poelarends, Structural and functional characterization of a macrophage migration inhibitory factor homologue from the marine cyanobacterium *Prochlorococcus marinus*, *Biochemistry.* 49 (2010) 7572–7581.
doi:10.1021/bi1008276.
- [23] H.M. Beyer, P. Gonschorek, S.L. Samodelov, M. Meier, W. Weber, M.D. Zurbriggen, AQUA cloning: A versatile and simple enzyme-free cloning approach, *PLoS One.* 10 (2015) 1–20. doi:10.1371/journal.pone.0137652.
- [24] X. Shi, L. Leng, T. Wang, W. Wang, X. Du, J. Li, C. McDonald, Z. Chen, J.W. Murphy, E. Lolis, P. Noble, W. Knudson, R. Bucala, CD44 Is the Signaling Component of the Macrophage Migration Inhibitory Factor-CD74 Receptor Complex, *Immunity.* 25 (2006) 595–606. doi:10.1016/j.immuni.2006.08.020.

- [25] S. Park, S. Sadegh-nasseritt, D.C. Wiley, Invariant chain made in *Escherichia coli* has an exposed N-terminal segment that blocks antigen binding to HLA-DR1 and a trimeric C-HLA-DR1 C-terminal that binds empty HLA-DR1, *Proc. Natl. Acad. Sci.* 92 (1995) 11289–11293.
- [26] A. Jasanoff, S.J. Park, D.C. Wiley, Direct observation of disordered regions in the major histocompatibility complex class II-associated invariant chain., *Proc. Natl. Acad. Sci. U. S. A.* 92 (1995) 9900–4. doi:10.1073/pnas.92.21.9900.
- [27] S. Günther, A. Schlundt, J. Sticht, Y. Roske, U. Heinemann, K.-H. Wiesmüller, G. Jung, K. Falk, O. Rötzschke, C. Freund, Bidirectional binding of invariant chain peptides to an MHC class II molecule, *Proc. Natl. Acad. Sci. U. S. A.* 107 (2010) 22219–24. doi:10.1073/pnas.1014708107.
- [28] A. Jasanoff, G. Wagner, D.C. Wiley, Structure of a trimeric domain of the MHC class II-associated chaperonin and targeting protein Ii. *EMBO J.* 17 (1998), 6812–6818
- [29] A. Jasanoff, S. Song, A.R. Dinner, G. Wagner, D.C. Wiley, One of two unstructured domains of Ii becomes ordered in complexes with MHC class II molecules, *Immunity.* 10 (1999) 761–768. doi:10.1016/S1074-7613(00)80075-8.
- [30] P. Ghosh, M. Amaya, E. Mellins, D.C. Wiley, The structure of an intermediate in class II MHC maturation: CLIP bound to HLA-DR3, *Nature.* 378 (1995) 457–62. doi:10.1038/378457a0.
- [31] C.A. Painter, M.P. Negroni, K.A. Kellersberger, Z. Zavala-Ruiz, J.E. Evans, L.J. Stern, Conformational lability in the class II MHC 310 helix and adjacent extended strand dictate HLA-DM susceptibility and peptide exchange, *Proc. Natl. Acad. Sci. U. S. A.* 108 (2011) 19329–34. doi:10.1073/pnas.1108074108.
- [32] J.R. Newcomb, C. Carboy-newcomb, P. Cresswell, Trimeric Interactions of the Invariant Chain and Its Association with Major Histocompatibility Complex Class II $\alpha\beta$ Dimers, *J. Bio. Chem.* 271 (1996) 24249–24256.
- [33] R. Meza-romero, G. Benedek, L. Leng, R. Bucala, P. Rd, O. Health, N. Haven, O. Health, Predicted structure of MIF/CD74 and RTL1000/CD74 complexes, *Metab. Brain Dis.* 31 (2016) 249–255. doi:10.1007/s11011-016-9798-x.
- [34] L. Schindler, N. Dickerhof, M.B. Hampton, J. Bernhagen, Post-translational regulation of macrophage migration inhibitory factor: Basis for functional fine-tuning, *Redox Biol.* 15 (2018) 135–142. doi:10.1016/J.REDOX.2017.11.028.
- [35] A. Kukol, J. Torres, I.T. Arkin, A Structure for the Trimeric MHC Class II-associated Invariant Chain Transmembrane Domain, *J. Mol. Biol.* 320 (2002) 1109–1117. doi:10.1016/S0022-2836(02)00563-6.
- [36] Ann M. Dixon, Bradford J. Stanley, Erin E. Matthews, and Jessica P. Dawson, Donald M. Engelman, Invariant Chain Transmembrane Domain Trimerization: A Step in MHC Class II Assembly, *Biochemistry.* 45 (2006). doi:10.1021/BI052112E.

A.



B.

MBP-sCD74

MKIEEGKLVIIWINGDKGYNGLAEVGKKFEKDTGIKVTVEHPDKLEEFQVAATGDGPDIIIFWAHDRFGGYAQSGLLAEITPDKAFQDKLYPFTWDAVRY
 NGKLIAYPIAVEALSIIYNKDLLPNPPKTWEEIPALDKELKAKGKSALMFNLQEPYFTWPLIAADGGYAFKYENKDYDKVDVGNAGAKAGLTFVLDLIKN
 KHMNADTDYSIAEAAFNGETAMTINGPWAWSNIDTSKVNYGVTVLPTFKGQPSKPFVGLSAGINAASPNKELAKEFLENLLTDEGLEAVNKDKPLG
 AVALKSYEEELAKDPRIATMENAQKGEIMPNIQMSAFWYAVRTAVINAASGRQTVDEALKDAQTNSSNNNNNNNNNNNLGIEGRISEFIEGRARLD
 KLTVTSQNLQLENLRMKLPKPPKPVSKMRMATPLLMQALPMGALPQGPMQNAKYGNMTEHDHVMHLLQNADPLKVYPPLKGSFPENLRHLKNT
 METIDWKVFESWMHHWLLFEMSRHSLEQKPTDAPPKESLELEDPSGLGVTKQDLGPVPMLEHHHHHHH

Fh8-sCD74

MQTGMPVSVQVEKLLHVLDRNGDGKVSAEELKAFADDSKCPDLSNKIKAFIKEHDKNKDGKLDLDELVSILSSGTSGLGGLVLFQGGPAMAASGSIGA
 NKLRDLKLTVTSQNLQLENLRMKLPKPPKPVSKMRMATPLLMQALPMGALPQGPMQNAKYGNMTEHDHVMHLLQNADPLKVYPPLKGSFPENLRHLKNTMETIDWKVFESWMHHWLLFEMSRHSLEQKPTDAPPKESLELEDPSGLGVTKQDLGPVPMLEHHHHHHH

Fh8-ssCD74

MQTGMPVSVQVEKLLHVLDRNGDGKVSAEELKAFADDSKCPDLSNKIKAFIKEHDKNKDGKLDLDELVSILSSGTSGLGGLVLFQGGPAMAASGSIGA
 NKLLMQALPMGALPQGPMQNAKYGNMTEHDHVMHLLQNADPLKVYPPLKGSFPENLRHLKNTMETIDWKVFESWMHHWLLFEMSRHSLEQKPTDAPPKESLELEDPSGLGVTKQDLGPVPMLEHHHHHHH

sssCD74

GPMQNAKYGNMTEHDHVMHLLQNADPLKVYPPLKGSFPENLRHLKNTMETIDWKVFESWMHHWLLFEMSRHSLEQKPTDAPPKESLELEDPSGLGVTKQDLGPVPMLEHHHHHHH

Figure 1. (A) Schematic presentation of human CD74 isoform p35 and CD74 proteins used in this study. IC = intracellular (residues 1-46), TM = transmembrane (residues 47-73), EC = extracellular (residues 74-232), the inverted triangles indicate where isoforms p33, p35, p41 and p43 differ. Xa = factor Xa cleavage site, 3C = 3C protease cleavage site, His₆ = (His)₆-tag. **(B) Amino acid sequences of CD74 proteins used in this study.** The sequences of the solubility enhancing peptides MBP and Fh8 are in italics, the proteolytic sites are underlined, and the CD74 sequences are presented in bold. Sequences of CD74 that are dotted or dashed underlined represent the CLIP region and the membrane-distal trimerisation domain, respectively.

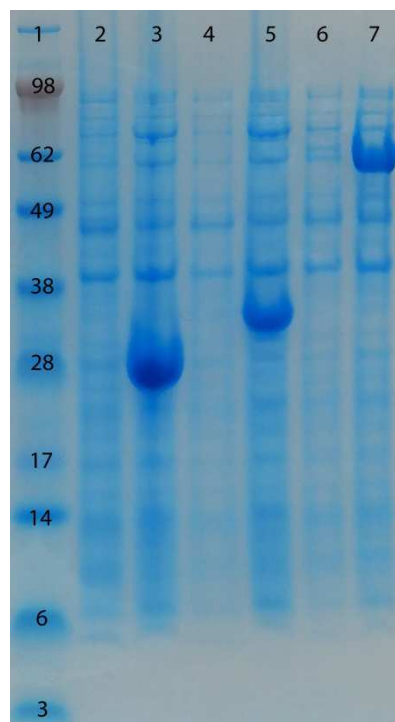


Figure 2. Overproduction of CD74 fusion proteins. Lane 1: marker proteins with the indicated molecular weights. Lanes 2 and 3: cell lysate before and after overproduction of Fh8-ssCD74 (MW 25.0 kDa), respectively. Lanes 4 and 5: cell lysate before and after overproduction of Fh8-sCD74 (MW 29.6 kDa), respectively. Lanes 6 and 7: cell lysate before and after overproduction of MBP-sCD74 (MW 62.3 kDa), respectively.

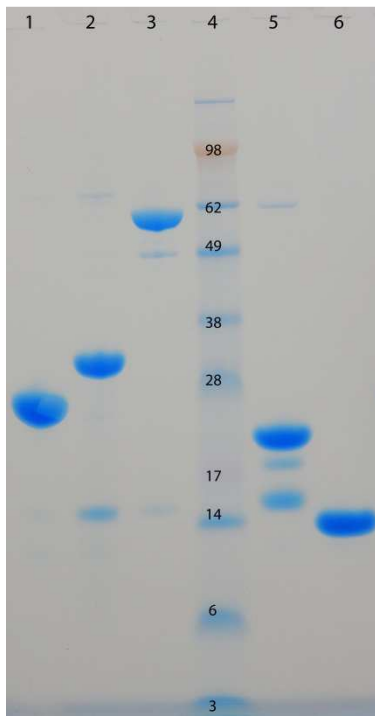


Figure 3. SDS gel of different purified CD74 proteins. Fh8-ssCD74 (lane 1), Fh8-sCD74 (lane 2), MBP-sCD74 (lane 3), sCD74 (lane 5), and sssCD74 (lane 6). Lane 4 contains the protein marker with indication of their molecular weights.

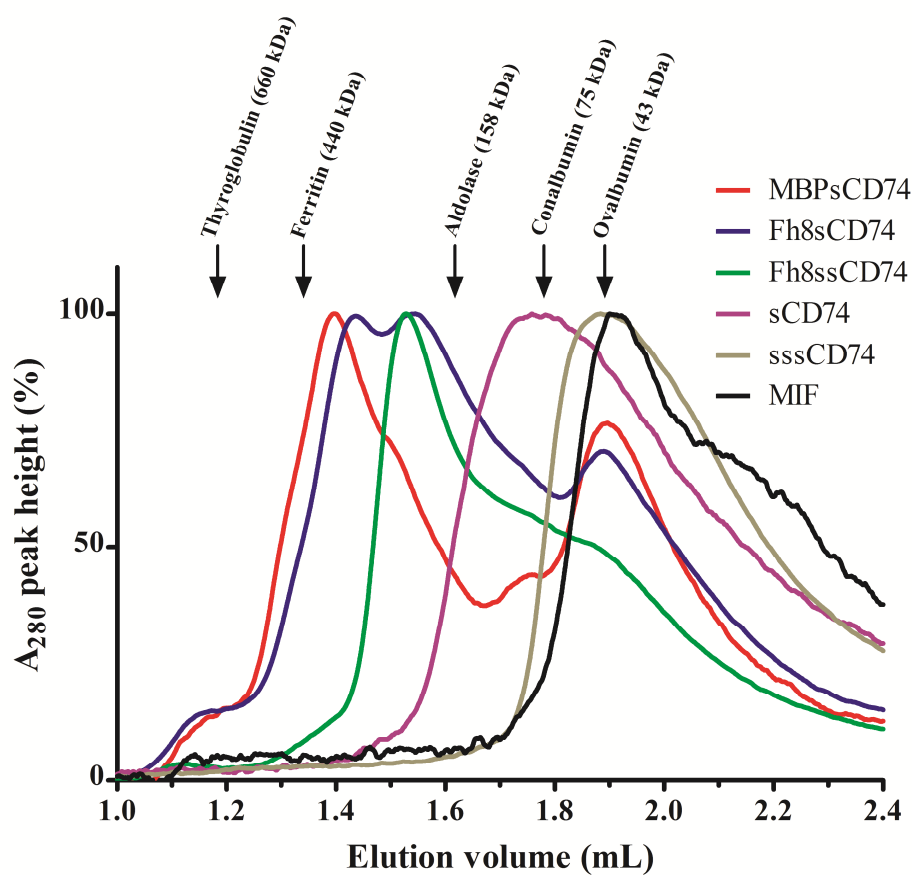


Figure 4. Size exclusion chromatography of MIF and sCD74 proteins on a Superdex200 5/150 column (GE Healthcare, The Netherlands). Purified proteins were separately analyzed on a 3 mL gel filtration column Superdex200 5/150 by injecting 20 μ l of a 1 mg/ml protein solution onto the column equilibrated with PBS, pH 7.4, at 10 $^{\circ}$ C. Each chromatogram was normalised to its absorbance at 280 nm. The column was also calibrated with 20 μ l of 1 mg/ml solutions of five marker proteins: thyroglobulin (669 kDa), ferritin (440 kDa), aldolase (158 kDa), conalbumin (73 kDa), and ovalbumin (43 kDa). The elution volumes of these marker proteins (1.19; 1.34; 1.61; 1.78; and 1.89 ml, resp.) are indicated with arrows.

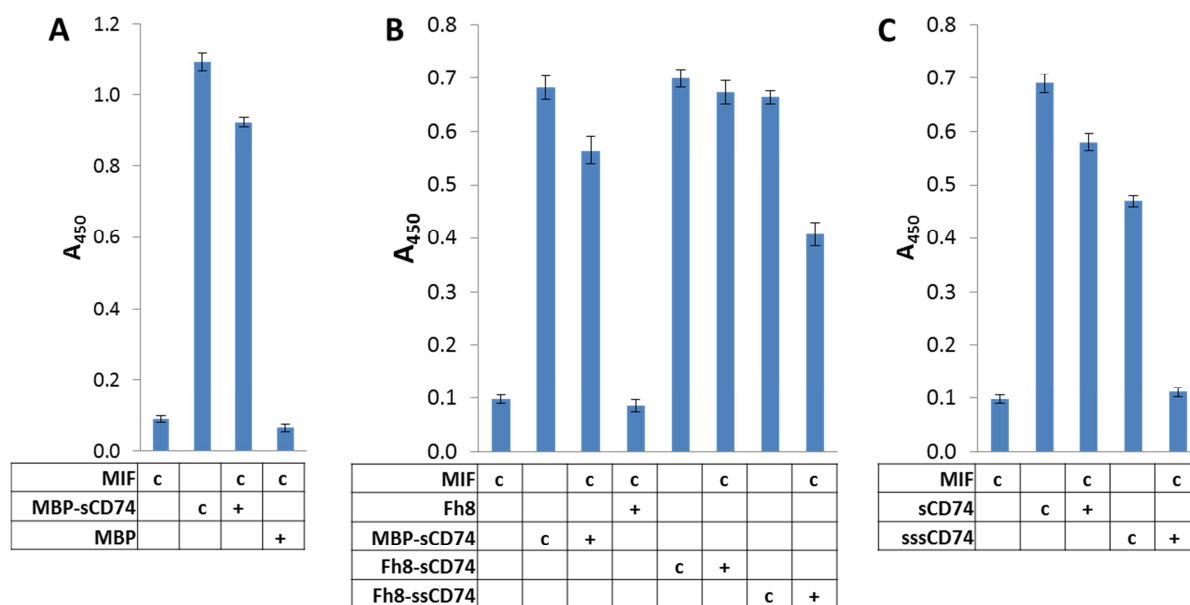


Figure 5. ELISA binding observation between MIF and sCD74 fusion proteins. (A) MIF with 500 nM MBP-sCD74 and controls using mouse anti-MBP mAb for detection (B) MIF with 500 nM MBP-sCD74, Fh8-sCD74 or Fh8-ssCD74 and controls using rabbit anti-CD74 pAb for detection. (C) MIF with 500 nM sCD74 or sssCD74 and controls using rabbit anti-CD74 pAb for detection. c: protein used for coating (300 nM MIF or 500 nM of other proteins); +: protein tested for binding to MIF

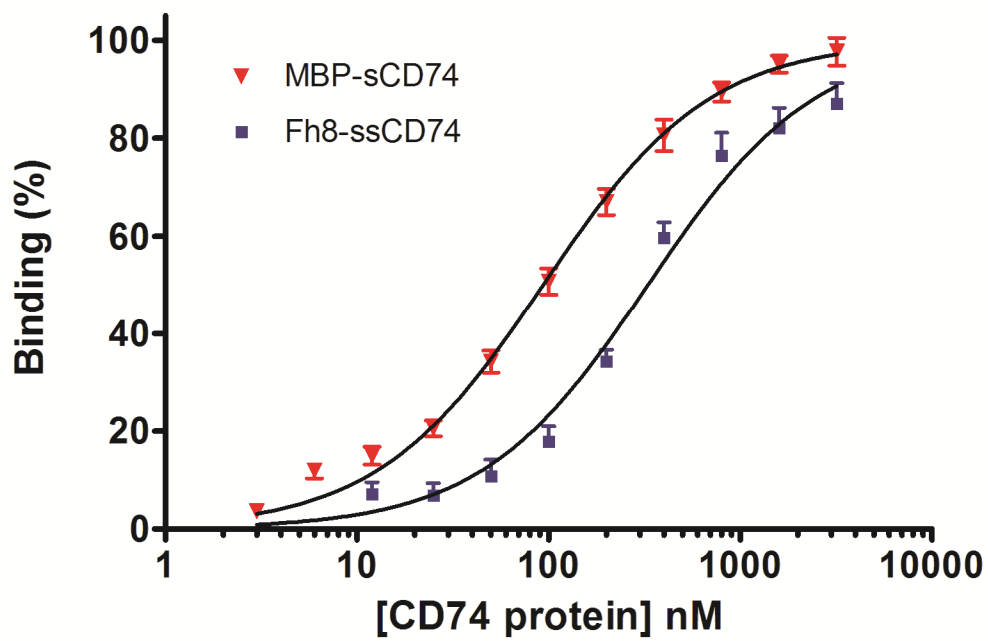


Figure 6. Dose-dependent ELISA of the interaction of 300 nM coated MIF with MBP-sCD74 or Fh8-ssCD74, revealed with α MBP or α CD74 antibodies, respectively.

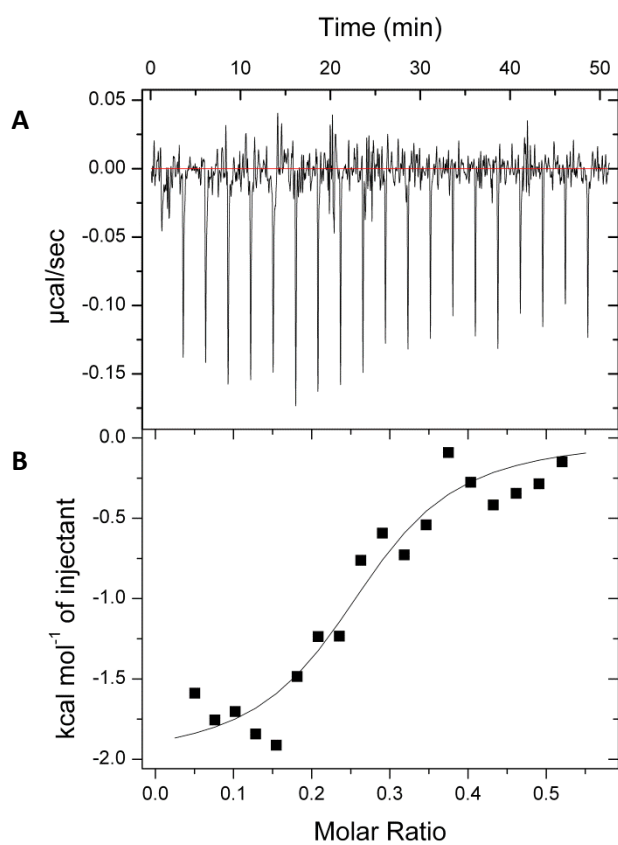


Figure 7. ITC binding kinetics measurement. A. Heat flow as a function of time. **B.** Reaction enthalpy versus molar ratio.

Highlights Kok et al:

- Solubility-enhancing peptides e.g. MBP and Fh8 greatly increase the yield in purified fusion proteins of human invariant chain CD74 constructs
- The membrane-distal trimerization domain of CD74 needs a sufficiently long N-terminal extension for high affinity binding to MIF, comprising at least amino acids 113-125